

Multi-wavelength measurements of aerosol optical absorption coefficients using a photoacoustic spectrometer

This content has been downloaded from IOPscience. Please scroll down to see the full text.

2014 Chinese Phys. B 23 064205

(<http://iopscience.iop.org/1674-1056/23/6/064205>)

View [the table of contents for this issue](#), or go to the [journal homepage](#) for more

Download details:

IP Address: 61.190.88.135

This content was downloaded on 23/07/2015 at 06:12

Please note that [terms and conditions apply](#).

Multi-wavelength measurements of aerosol optical absorption coefficients using a photoacoustic spectrometer*

Liu Qiang(刘 强)^{a)b)}, Huang Hong-Hua(黄宏华)^{b)}, Wang Yao(王 尧)^{c)}, Wang Gui-Shi(王贵师)^{b)d)}, Cao Zhen-Song(曹振松)^{b)}, Liu Kun(刘 锟)^{b)d)}, Chen Wei-Dong(陈卫东)^{e)}, and Gao Xiao-Ming(高晓明)^{b)d)†}

^{a)}Department of Optics & Optical Engineering, University of Science and Technology of China, Hefei 230026, China

^{b)}Key Laboratory of Atmospheric Composition and Optical Radiation, Chinese Academy of Sciences, Hefei 230031, China

^{c)}Institute for Environmental Reference Materials, Ministry of Environmental Protection, Beijing 100029, China

^{d)}Laboratory of Atmospheric Physico-Chemistry, Anhui Institute of Optics & Fine Mechanics, Chinese Academy of Sciences, Hefei 230031, China

^{e)}Laboratoire de Physicochimie de l'Atmosphère, Université du Littoral Côte d'Opale, 189A, Av. Maurice Schumann, 59140 Dunkerque, France

(Received 19 August 2013; revised manuscript received 27 November 2013; published online 10 April 2014)

The atmospheric aerosol absorption capacity is a critical parameter determining its direct and indirect effects on climate. Accurate measurement is highly desired for the study of the radiative budget of the Earth. A multi-wavelength (405 nm, 532 nm, 780 nm) aerosol absorption meter based on photoacoustic spectroscopy (PAS) involving a single cylindrical acoustic resonator is developed for measuring the aerosol optical absorption coefficients (OACs). A sensitivity of 1.3 Mm^{-1} (at 532 nm) is demonstrated. The aerosol absorption meter is successfully tested through measuring the OACs of atmospheric nigrosin and ambient aerosols in the suburbs of Hefei city. The absorption cross section and absorption Ångström exponent (AAE) for ambient aerosol are determined for characterizing the component of the ambient aerosol.

Keywords: photoacoustic spectrometer, atmospheric aerosols, absorption coefficient, absorption Ångström exponent

PACS: 42.62.Fi, 42.68.Jg, 42.25.Bs

DOI: 10.1088/1674-1056/23/6/064205

1. Introduction

Apart from the negative effect on human health and visibility, atmospheric aerosols also play a key role in the global climate system by its direct effects (scattering and absorption of the solar radiation)^[1] and indirect effects (modification of cloud properties and abundance)^[2,3] on climate. Among these factors, aerosol absorption is of particular importance for both direct and indirect aerosol effects.^[4,5] Unfortunately, aerosol absorption is one of the most uncertain parameters in the above-mentioned effects and also it is one of the most difficult quantities to measure.^[6]

An optical absorption coefficient (OAC) α ($[\alpha] = \text{Mm}^{-1} = 10^{-8} \text{ cm}^{-1}$) is used to characterize the magnitude of aerosol absorption. Generally, approaches to determining aerosol OAC can be classified into two categories: filter-based techniques, and filter-free *in situ* techniques. Instruments based on filter-based techniques, such as the aethalometer, multi-angle absorption photometers (MAAP), the continuous soot monitoring system (COSMOS), and particle soot absorption photometer (PSAP), are subjected to the fact that the reliability of the measured data is limited, due primarily to artifacts such as filter-aerosol interactions (especially multiple scattering), the shadowing of the incident light, which intensifies with the increase of filter loading and aerosol scattering effect.^[7-9] The SP2 (single particle soot photometer (SP2) instrument, based

on laser-induced incandescence (LII) measurement), is usually used for filter-free *in situ* characterization of strong aerosol light absorption. The main disadvantage of this technique is the influence of the heating, owing to the high power density laser beam, on particle composition and morphology.^[10,11] Another filter-free *in situ* approach is based on the measurement of the total aerosol extinction coefficient by cavity ring-down spectroscopy (CRDS)^[12] and the scattering coefficient with an integrating nephelometer,^[13] and then the OAC is deduced by subtracting the scattering coefficient from the extinction coefficient. However, as the absorption coefficient is determined from a small difference between two large quantities, this approach is rather suited for high pollution events, or laboratory studies with high aerosol concentration.^[14,15]

The photoacoustic spectroscopy (PAS) technique for observing the aerosols in their natural suspended states, is commonly recognized as one of the best candidates to measure the OAC of aerosols. The PAS technique was first employed to measure the light absorption of aerosols in the late 1970's.^[16,17] Haisch *et al.*^[18] developed a mobile PAS sensor consisting of two differential PA cells for on-line monitoring of the soot emission in diesel exhaust gas. The limit of detection was found to be $2\text{-}\mu\text{g}\cdot\text{m}^{-3}$ black carbon (BC) for diesel soot in exhaust gas and $10 \mu\text{g}\cdot\text{m}^{-3}$ for artificial soot (13.2 Mm^{-1} and 66 Mm^{-1} respectively on the assump-

*Project supported by the Open Research Fund of Key Laboratory of Atmospheric Composition and Optical Radiation, Chinese Academy of Sciences, and the National Natural Science Foundation of China (Grant Nos. 41175036 and 41205120).

†Corresponding author. E-mail: xmgao@aiofm.ac.cn

tion that an optical absorption efficiency is $10 \text{ m}^2 \cdot \text{g}^{-1}$ at 532 nm and an absorption Ångström exponent is 1 for BC).^[18] Arnott *et al.*^[19] and Lewis *et al.*^[20] designed a PAS with a U-shape resonator in order to simultaneously measure light absorption with a microphone and scattering with a cosine-weighted sensor. Aerosol absorption measurements using this PAS have been reported at wavelengths 355 nm, 405 nm, 532 nm, 671 nm, 781 nm, 870 nm, and 1047 nm respectively for laboratory-generated and ambient aerosols.^[21,22] Multi-wavelength operation of a PAS system has already been demonstrated to be a useful method of studying spectral properties of aerosol optical absorption. Arnott's PAS was employed for dual-wavelength (405 nm and 870 nm) measurements of biomass burning emissions.^[20] Tibor *et al.*^[23] reported on a multi-wavelength PAS instrument equipped with four identical PA cells operating at four wavelengths generated from an Nd:YAG disc laser with a fundamental wavelength of 1064 nm and harmonics at 532, 355, and 266 nm). Minimum detectable OAC was determined to be 0.7 Mm^{-1} at 1064 nm, 2.3 Mm^{-1} at 532 nm, 8.93 Mm^{-1} at 355 nm, and 11 Mm^{-1} at 266 nm.^[24]

In this paper, we present a multi-wavelength (405, 532, 780 nm) aerosol absorption meter based on PAS involving a single cylindrical acoustic resonator (operating in its first longitudinal mode) for measuring the aerosol OACs. NO_2 absorption spectrum at 532 nm is used for PA resonator calibration. Measurements of OACs of laboratory aerosol and ambient aerosol are carried out to evaluate the performance of the developed aerosol absorption meter. The absorption cross section and absorption Ångström exponent are determined to characterize the component of the ambient aerosol.

2. Experimental setup

The experimental setup is schematically shown in Fig. 1. A detailed description of this apparatus is given elsewhere^[25]

in Chinese. The optical sources included a frequency-doubled Nd:YAG laser emitting at 532 nm and two diode lasers emitting at 405 nm and 780 nm, respectively. Laser beams were amplitude-modulated through a TTL signal from a function generator. The average powers of the lasers were about 195 mW, 83 mW, and 800 mW, respectively. The light beams were coupled together and directed into the PA cell by means of two mirrors (M_1 , M_4) and two dichroic mirrors (M_2 , M_3). The PA cell, made of duralumin, consisted of a central cylindrical resonator (length = 100 mm, radius = 9 mm) and two buffer volumes (about half the length of the resonator with a radius of 40 mm) for filtering acoustic noise. The windows of the PA cell were sealed with quartz glass. The PA signal was detected by a miniature electret microphone (MP201, Institute of Acoustics, the Chinese Academy of Sciences) which was inserted into the middle of the resonator and demodulated with a lock-in amplifier (SR850, Stanford Research Systems). The time constant of the lock-in amplifier was set to be 1 s in combination with an 18-dB/octave slope filter (the corresponding bandwidth was 0.094 Hz). The output signals from the lock-in amplifier were acquired by a data acquisition card (AC-6115, W & WLAB). The transmitted laser beams emanating from the PA cell were monitored by an optical power meter (EPM2000, Coherent) to normalize the PA signals respectively.

A scanning mobility particle sizer (SMPS, 3936, TSI) consisting of a differential mobility analyzer (DMA, 3080, TSI) and a condensation particle counter (CPC, 3022A, TSI), was placed downstream to measure the size distribution and number concentration of the samples. Aerosol samples were dragged through the PA cell by the CPC internal-located pump. The whole experimental process was controlled via a program based on Labview software (National Instrument).

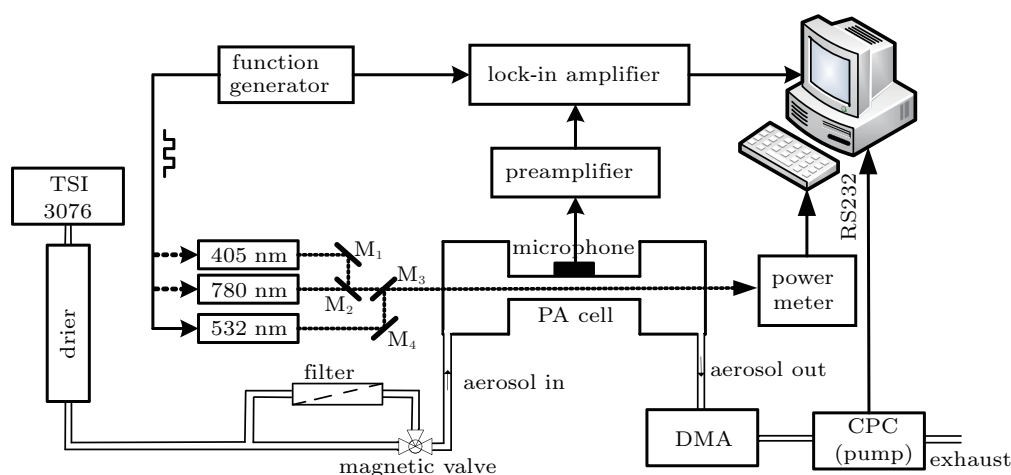


Fig. 1. Schematic diagram of the experimental setup.

3. Results and discussion

3.1. Resonant frequency and quality factor of the PA cell

Characterization of the PA cell resonant frequency is performed using the NO₂ absorption signal. The PA response is measured as a function of the amplitude modulation frequency. The measurement is carried out at room temperature (296 K) and standard atmospheric pressure. The acoustic resonance frequency is found to be $f_0 \approx 1617$ Hz, corresponding to a quality factor of 21. The low quality factor is of benefit to reducing the influence of resonant frequency drift caused by the variation of temperature and humidity in the sampled air.

3.2. Calibration of aerosol OAC

The calibration method of aerosol OAC described by Arnott *et al.*^[26] and Tibor *et al.*^[23] is used in the present work. Absorption of NO₂ gas at 532 nm is used to calibrate the measurement of aerosol OAC. Figure 2 shows the broad absorption band of NO₂ near 532 nm and the emission spectrum of the solid green laser used in our system at room temperature. Based on the HITRAN 2008 database,^[27] NO₂ exhibits an absorption cross section of about 1.5×10^{-19} cm²/molecule at 532 nm. The emission spectrum is centered at 532.4 nm with a spectral width (FWHM) of about 0.74 nm. According to the PA theory, the generated acoustic signal can be expressed as

$$S = P \times M \times C_{\text{cell}} \times \alpha_0 \times c + S_b, \quad (1)$$

where S ($[S] = \text{V}$) is the amplitude of the PA signal, P ($[P] = \text{W}$) is the average laser power at the resonant frequency, M ($[M] = \text{V} \cdot \text{Pa}^{-1}$) is the microphone sensitivity, C_{cell} ($[C] = \text{Pa} \cdot (\text{cm}^{-1} \cdot \text{W})^{-1}$) is the cell constant, α_0 is the specific absorption coefficient of the sample ($[\alpha_0] = \text{Mm}^{-1}/(\text{g/m}^3)$ for aerosol and $[\alpha_0] = \text{Mm}^{-1}/\text{ppbv}$ for gas), c is the concentration of the sample ($[c] = \text{g/m}^3$ for aerosol and $[c] = \text{ppbv}$ for gas), and S_b is the background acoustic signal ($[S_b] = \text{V}$). The quantity $\alpha_0 \times c$ equals OAC. So, it is possible to determine the product of M and C if the α_0 is known (based on a calibration with known NO₂ concentration). The relationship between OAC of the calibration gas and the concentration c is given by

$$\alpha_0 \times c = N_L \frac{p}{T} c \cdot \sigma(\lambda), \quad (2)$$

where p and T are the pressure and temperature of the sample gas respectively, $\sigma(\lambda)$ is the wavelength-dependent absorption cross section ($[\sigma] = \text{cm}^2/\text{molecule}$), $N_L = 2.68 \times 10^{19}$ mol·cm⁻³·atm⁻¹ (1 atm = 1.01325 × 10⁵ Pa) is the Loschmidt number at 273.5 K and 1 atm. The α_0 can thus be expressed as

$$\alpha_0 = 2.68 \times 10^{19} \frac{273.5}{T} p \cdot \sigma(\lambda). \quad (3)$$

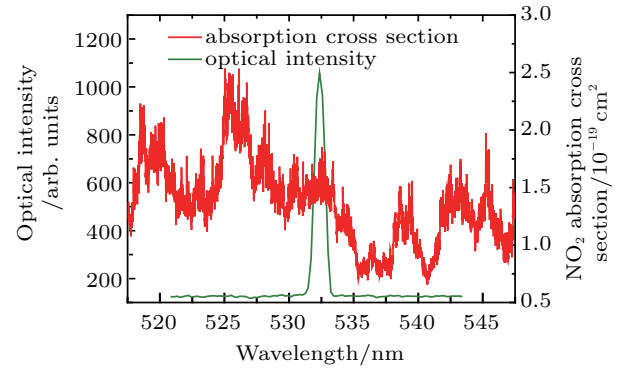


Fig. 2. (color online) Absorption spectrum of NO₂ at 532 nm associated with the solid laser emission spectrum used in the present work.

In a method different from that used in previous work,^[25] $\sigma(\lambda)$ is calculated as follows. In the case of using a broadband light source, $\sigma(\lambda)$ can be defined as

$$\sigma(\lambda) = \sum_{i=1}^n \sigma(\lambda_i) \cdot g(\lambda_i) \quad (4)$$

with $\sigma(\lambda_i)$ being the absorption cross section at λ_i (λ_i is restricted in the laser emission region, $[\lambda_i] = \text{nm}$) and $g(\lambda_i)$ the normalized function ($\sum_{i=1}^n g(\lambda_i) = 1$) for the wavelength-dependent optical power density distribution. In Eq. (4), the values of $\sigma(\lambda_i)$ are provided by the HITRAN 2008 database, and the $g(\lambda_i)$ function is deduced from the measurement by use of a high-resolution optic spectrometer (Ocean Optics Inc., HR2000). The α_0 value is found to be $0.37 \text{ Mm}^{-1}/\text{ppbv}$ in the present PA spectrometer. In the calibration process, the PA cell was purged with NO₂ gas buffered in nitrogen with known concentrations (in the present case, 200, 300, 400, 500 ppbv) and the acquired PA signals are divided by the laser power and linearly fitted as shown in Fig. 3. The noise measured in the case of a non-absorbing gas sample (pure N₂) is 0.13 nV/mW (1σ) and the minimum detectable OAC is found to be 1.3 Mm^{-1} . The corresponding normalized noise equivalent absorption (NNEA) coefficient can be determined by^[28]

$$\text{NNEA} = \frac{\alpha_{\text{min}} P}{\sqrt{\Delta f}}, \quad (5)$$

where α_{min} ($[\alpha_{\text{min}}] = \text{Mm}^{-1}$) is the minimum detectable OAC, P ($[P] = \text{W}$) is the average laser power, and Δf ($[\Delta f] = \text{Hz}$) is the equivalent noise detection bandwidth. The NNEA coefficient of the PA spectrometer is calculated to be $8.2 \times 10^{-9} \text{ W} \cdot \text{cm}^{-1} \cdot \text{Hz}^{-1/2}$.

According to Arnott's and Tajai's work, the calibration results of aerosol OAC are independent of the determined wavelength, so the PAS is able to make aerosol OAC measurements at the other two wavelengths (405 nm and 780 nm) with this calibration result.

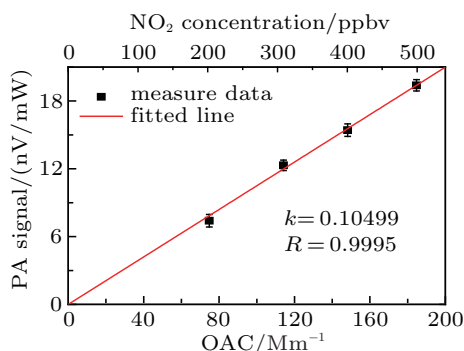


Fig. 3. (color online) Result of the calibration of aerosol OAC.

3.3. Measurements of aerosol OAC

In OAC measurements of atmospheric aerosols, interference from gas absorption, especially NO_x and water-vapor absorption,^[27] should be considered. In our experiments, the PA signal of particle free air is repeatedly measured and used as background signal S_b . By subtracting S_b from the PA signal S of sampled air, the gas absorption interference is removed along with the acoustic noise.

3.3.1. Laboratory generated aerosol

In order to make a performance evaluation of the developed PA spectrometer, aerosol is generated in our laboratory with an aerosol generator (3076, TSI) through using a solution of nigrosin dye ($\text{C}_{48}\text{N}_9\text{H}_{51}$) in deionized water. The particles are dried through a diffusion drier. The relative humidity (RH) is controlled to be less than 5%, well below the RH at which any effect of evaporation on the acoustic signal is expected.^[29] Figure 4 shows the size distribution of the nigrosin aerosol, measured with an SMPS. The concentration of the solution used in the experiment is 50 mg/L, and the peak of the particle concentration is found to be at an aerosol diameter of 57 nm. The nigrosin aerosol is then diluted with particle free air to different concentrations. The concentration of the particles passed through the PA cell is monitored by a CPC which is located at the end of the stream and the aerosol sample is dragged by the internal-located pump.

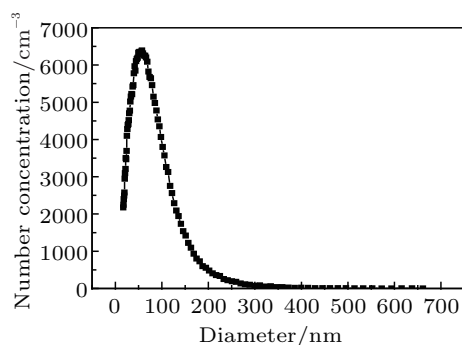


Fig. 4. Size distribution of the laboratory-generated nigrosin aerosol.

Aerosol OAC can be expressed as

$$\text{OAC} = N \cdot \sigma, \quad (6)$$

where N and σ are the particle number concentration and the particle absorption cross section respectively. OACs of the nigrosin aerosol at different concentrations are shown in Fig. 5. The slope of the linear fitting, recognized as the absorption cross section, is found to be $2.09 \times 10^{-11} \text{ cm}^2$, which accords well with the result (of $1.8 \times 10^{-11} \text{ cm}^2$) obtained by Arthur and Jeonghoon^[30] through using a photothermal interferometric spectrometry.

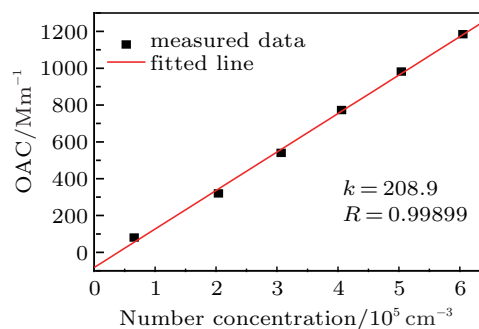


Fig. 5. (color online) OACs of the nigrosin aerosol at different number concentrations.

3.3.2. Environmental aerosol

The developed PAS instrument is then used to measure the ambient aerosol absorption. The data of ambient aerosol mentioned in this paper are all sampled near the edge of a lake (in a suburban of Hefei city). In this area, the main source of absorbing aerosol (black carbon, BC) is the vehicle exhaust released from the traffic within 300 m of the sample inlet. Sampling is carried out at $\sim 5 \text{ m}$ above the ground at the second floor of the laboratory. Figure 6 shows a time series of 12 hour (from 21:00 on August 28th to 9:00 on August 29th) monitoring of the OAC at 532 nm and the particle concentration of the ambient aerosol. In the process of sampling, it was cloudy and the ambient temperature was between 296 K and 301 K. The variation trend of the OAC is in accordance with that of the number concentration in the traffic free time period (before 6:30 am). The OAC increased from $\sim 20 \text{ Mm}^{-1}$ up to $\sim 35 \text{ Mm}^{-1}$ quickly after 6:30 am because there was a traffic jam on the road nearby. At 8:30 am, aerosol particles were removed from the air by a filter and the OAC was down to \sim zero. On another sunny clear day, a time series measurement of the ambient aerosol OAC was carried out and the result is given in Fig. 7(a), aerosol size distribution and the absorption cross section are also given in Figs. 7(b) and 7(c), the peak of the particle concentration is found to be at an aerosol diameter of $\sim 109 \text{ nm}$ and the absorption cross section is found to be $3.49 \times 10^{-12} \text{ cm}^2$. According to Arthur and Jeonghoon's results,^[30] the BC absorption cross section primarily varies as the square of the particle radius. The results indicate that less BC components exist in the sampled aerosol in the traffic free time period.

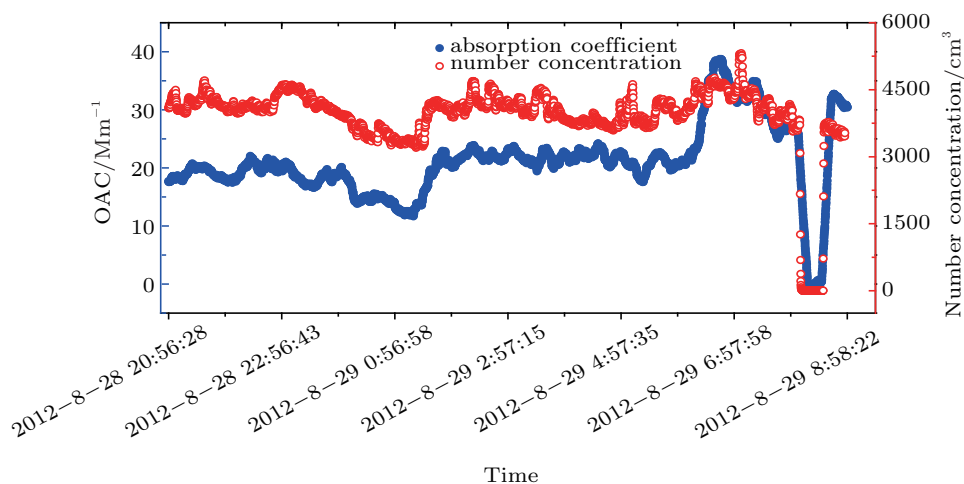


Fig. 6. (color online) Real-time measurement of the OAC at 532 nm and the number concentration of the ambient aerosol.

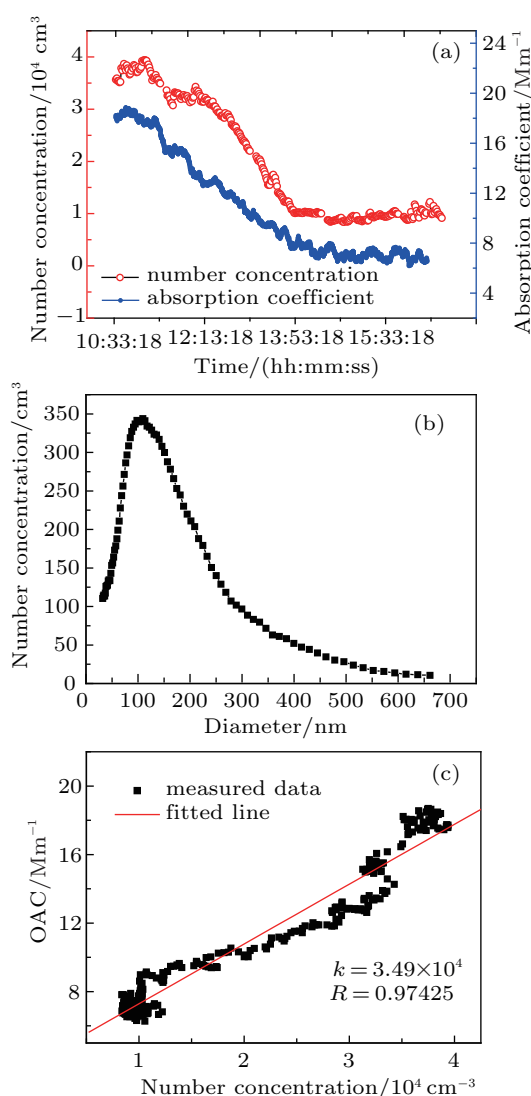


Fig. 7. (color online) (a) OAC time series measurement at 532 nm on a sunny clear day; (b) size distribution of the measured ambient aerosol; (c) plot of the measured OAC at 532 nm versus the particle number concentration.

Based on the measurements of OAC at triple wavelengths, the wavelength-dependent OAC is studied. As shown in Fig. 8,

the wavelength dependence of OAC can be expressed by a power law^[24]

$$\text{OAC} = a \cdot \lambda^{-b}, \quad (7)$$

where a is a wavelength-independent constant, λ is the wavelength, and b is the parameter called absorption Ångström exponent (AAE). A value of AAE = 1 implies a wavelength-independent refractive index for BC and a much smaller particle size than the wavelength,^[31] e.g. vehicle exhaust. OACs at 405 nm, 532 nm, and 780 nm are measured by introducing each light beam into the PA cell in turn. An OAC measurement at each wavelength is made for 5 minutes and the whole procedure is completed in 15 minutes. Particle number concentration is synchronously measured in order to unify OAC measurement to the same particle number concentration. The result is plotted versus wavelength in Fig. 8. A fitting of Eq. (6) to the measured data yields an AAE value of 2.04. This strong wavelength-dependent absorption (AAE > 1.6) indicates a dominant organic carbon absorption (e.g. brown carbon, BrC)^[32–34] in our observation.

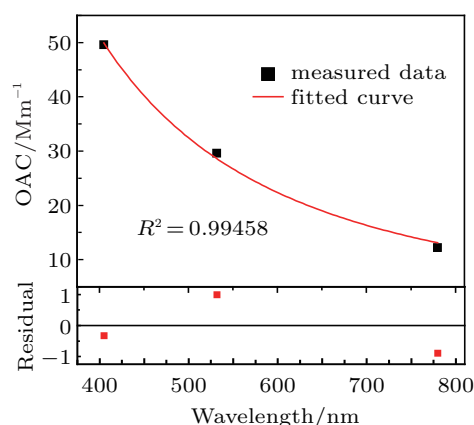


Fig. 8. (color online) Measured wavelength-dependent ambient aerosol OAC.

4. Conclusion

A multi-wavelength PA spectrometer is developed for investigating the optical absorption properties of aerosols. The instrument is based on a cylindrical acoustic resonator involving three lasers emitting at 405 nm, 532 nm, and 780 nm respectively. The calibration for the accurate measurement of the OAC is achieved using the NO₂ reference sample, at 532 nm. The minimum detectable OAC is found to be 1.3 Mm⁻¹ with a normalized noise equivalent absorption (NNEA) coefficient of $8.2 \times 10^{-9} \text{ W}\cdot\text{cm}^{-1}\cdot\text{Hz}^{-1/2}$. This corresponds to a minimum detectable mass concentration of about 0.13 μg·m⁻³ for black carbon aerosol. The system is tested by laboratory generated nigrosin aerosol, and the result is in good agreement with that reported in the references. The developed instrument is then employed for measuring the OAC of ambient aerosol. Based on the multi-wavelength measurements of OAC, the absorption Ångström exponent parameter is determined, which allows determination of the aerosol nature. The obtained results imply the possibility of achieving a compact, wide spectra covered aerosol absorption meter required in field measurements.

Acknowledgment

We are greatly indebted to professor Gong Zhi-Ben for the helpful discussion and manuscript revision.

References

- [1] Schulz M, Textor C, Kinne S, Balkanski Y, Bauer S, Bernsten T, Berglen T, Boucher O, Dentener F, Guibert S, Isaksen I, Iversen T, Koch D, Kirkevåg A, Liu X, Montanaro V, Myhre G, Penner J, Pitari G, Reddy S, Seland Ø, Stier P and Takemura 2006 *Atmos. Chem. Phys.* **6** 5225
- [2] Wang H H and Sun X M 2012 *Chin. Phys. B* **21** 054204
- [3] Han Y, Wang T J, Rao R Z and Wang Y J 2008 *Acta Phys. Sin.* **57** 7396 (in Chinese)
- [4] Stier P, Seinfeld J H, Kinne S and Boucher O 2007 *Atmos. Chem. Phys.* **7** 5237
- [5] Si F Q, Liu J G, Xie P H, Zhang Y J, Liu W Q, Hiroaki K, Liu C, Nofel L and Nobuo T 2005 *Chin. Phys.* **14** 2360
- [6] Lack D A, Tie X X, Bofinger N D, Wiegand A N and Madronich S 2004 *J. Geophys. Res.* **109** D03203
- [7] Weingartner E, Saathoff H, Schnaiter M, Streit N, Bitnar B and Baltensperger U 2003 *J. Aerosol Sci.* **34** 1445
- [8] Petzold A, Busen R, Schröder F P, Baumann R, Kuhn M, Ström J, Hagen D E, Whitefield P D, Baumgardner D, Arnold F, Borrmann S and Schumann U 1997 *J. Geophys. Res.* **102** D25
- [9] Arnott W P, Hamasha K, Moosmüller H, Sheridan P J and Ogren J A 2005 *Aerosol Sci. Technol.* **39** 17
- [10] Vander W R, Tichich T M and Stephens A B 1998 *Appl. Phys. B* **67** 115
- [11] Vander W R and Choi M Y 1999 *Carbon* **37** 231
- [12] Smith J D and Atkinson D B 2001 *Analyst.* **126** 1216
- [13] Varma R, Moosmüller H and Arnott W P 2003 *Opt. Lett.* **28** 1007
- [14] Tibor Ajtai, Ágnes Filtp, Noémi Utry, Martin Schnaiter, Claudia Linke, Zoltán Bozóki, Gábor Szabó and Thomas Leisner 2011 *J. Aerosol Sci.* **42** 859
- [15] Moosmüller H, Chakrabarty R K and Arnott W P 2009 *J. Quant. Spectrosc. Radiat. Transfer* **110** 844
- [16] Bruce C W and Pinnick R G 1977 *Appl. Opt.* **16** 1762
- [17] Terhune R W and Anderson J E 1977 *Opt. Lett.* **1** 70
- [18] Beck H A, Niessner R and Haisch C 2003 *Anal. Bional. Chem.* **375** 1136
- [19] Arnott W P, Moosmüller H, Rogers C F, Jin T and Bruch R 1999 *Atmos. Environ.* **33** 2845
- [20] Lewis K, Arnott W P, Moosmüller H and Wold C E 2008 *J. Geophys. Res.* **113** D16203
- [21] Gyawali M, Arnott W P, Zaveri R A, Song C, Moosmüller H, Liu L, Mishchenko M I, Chen L W A, Green M C, Watson J G and Chow J C 2012 *Atmos. Chem. Phys.* **12** 2587
- [22] Arnott W P, Zielinska B, Rogers C F, Sagebiel J, Park K, Chow J, Moosmüller H, Watson J G, Kelly K, Wanger D, Sarofim A, Lighty J and Palmer G 2005 *Environ. Sci. Technol.* **39** 5398
- [23] Tibor Ajtai, Ágnes Filtp, Martin Schnaiter, Claudia Linke, Marlen Vragel, Zoltán Bozóki, Gábor Szabó and Thomas Leisner 2010 *J. Aerosol Sci.* **41** 1020
- [24] Tibor Ajtai, Ágnes Filtp, Gabriella Kecskeméti, Béla Hopp, Zoltán Bozóki and Gábor Szabó 2010 *Appl. Phys. A* **103** 1165
- [25] Liu Q, Niu M S, Wang G S, Cao Z S, Liu K, Chen W D and Gao X M 2013 *Spectrosc. Spect. Anal.* **33** 1729 (in Chinese)
- [26] Arnott W P, Moosmüller H and Walker J W 2000 *Rev. Sci. Instrum.* **71** 4545
- [27] The HITRAN database can be found at <http://www.hitran.com>
- [28] Elia A, Franco C D, Spagnolo V, Lugarà P M and Scarmarcio G 2009 *Sensors* **9** 2697
- [29] Arnott W P, Moosmüller H, Sheridan P J, Ogren J A, Raspet R, Slaton W V, Hand J L, Kreidenweis S M and Collett J L 2003 *J. Geophys. Res.* **108** 4034
- [30] Arthur Sedlacek and Jeonghoon Lee 2007 *Aerosol Sci. Tech.* **41** 1089
- [31] Bergstrom R W, Russell P B and Hignett 2002 *J. Atmos. Sci.* **59** 567
- [32] Bond T C, Bergstrom R W 2006 *Aerosol Sci. Tech.* **40** 27
- [33] Gyawali M, Arnott W P, Lewis K and Moosmüller H 2009 *Atmos. Chem. Phys.* **9** 8007
- [34] Flowers B A, Dubey M K, Mazzoleni C, Stone E A, Schauer J J, Kim S W and Yoon S C 2010 *Atmos. Chem. Phys.* **10** 10387